Resonant Frequency and Q of an Open-Ended Rectangular Cavity

DAVID M. POZAR, STUDENT MEMBER, IEEE

Abstract—**A field analysis of the TE_{10m} resonant mode in an open-ended rectangular cavity is presented. The cavity geometry consists of rectangular waveguide with thick H-plane bifurcations for the terminations at each end. The bifurcation problem is solved by the method of modal analysis and a resonance criterion is established. Expressions for the cavity fields are written and used to compute stored energy, power lost, and Q. Calculated values for resonant frequency and Q are given and compared with experimental data.**

I. Introduction

OPEN-ENDED microwave cavities find application where free flow of fluids through the cavity is desired, as in a refractometer. Gilmer and Thorn [1] have experimentally investigated various cavities of this type, while Wenger [2] has presented an analysis for the resonant frequency of a circular open-ended cavity.

The rectangular open-ended cavity is shown in Fig. 1. The rectangular waveguide size is chosen according to the microwave band of interest so that the TE_{10} is the only propagating mode. Resonance of the dominant mode takes place between the vanes with the fields in the termination regions consisting only of quickly decaying evanescent modes. Practically no energy is lost through the open terminations if they are at least a few wavelengths long.

In this paper the resonant frequency, fields, stored energies, power lost per cycle, and Q are found for the TE_{10m}, $m = 1, 2, 3 \cdots$, resonant mode of the open-ended rectangular cavity. Section II deals with solving the H-plane bifurcation problem which consists of determining the complex reflection coefficient ρ of the dominant mode and the coefficients of the forward and back-scattered evanescent modes which are excited by the discontinuity. When the bifurcating vane is of zero thickness ($t = 0$) an exact solution is possible by the Wiener–Hopf method, as in Collin [3], or by a residue calculus method, as in Mittra and Lee [4]. Wenger [2] solves the analogous circular cylindrical open-ended cavity by a Wiener–Hopf method. The method of solution employed here is modal analysis, closely following Wexler [5]. While it is an approximate method, it provides high accuracies quickly, with the advantage of being useful for the case where $t \neq 0$.

The phase of ρ is used in Section III to establish a resonance condition from which can be found the distance d between the vanes that is required for a given resonant frequency. In Section IV the total $\bar{E}$ and $\bar{H}$ fields in the cavity are found from superposition of H-plane bifurcation solutions of each termination, along with resonance condition information. These fields are plotted in three dimensions (E,H versus x,z) for a clearer presentation of the field solution, in particular the singularities of H_x and H_z at the vane edges. The field expressions are used in Section V to compute time-average stored electric and magnetic energies and power lost per cycle in the cavity walls. From this the unloaded cavity Q is calculated.

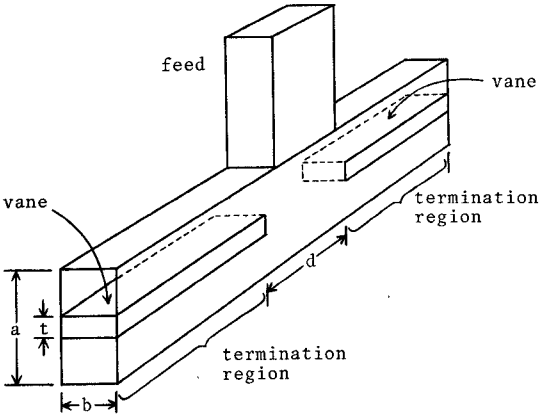

Fig. 1. Rectangular open-ended cavity design.

This method of solution is found to give accurate results for resonant frequencies, fields, and stored energies. However, the power loss (and hence Q) calculation is poorly convergent for thin vanes.

II. H-Plane Bifurcation Solution

The H-plane bifurcation geometry, shown in Fig. 2, consists of a vane of thickness t centered in the broad side of the waveguide. A TE_{10} wave is assumed to be incident from $z < 0$ and is considered to be the only propagating mode. All modes in the termination region ($z > 0$) are assumed to be evanescent. Due to the TE_{10} excitation the fields will consist of E_y, H_x, and H_z components. Since neither the excitation nor the cavity geometry contain any y variation, none of the fields will vary with y.

The modal analysis method begins by using the fact that the normal waveguide modes form a complete set in the guide cross section. Thus any arbitrary field can be expressed as a linear combination of the normal modes. If a unit amplitude incident E_y field is assumed, the total E_y field can be written as (assuming $\exp(j\omega t)$ time dependence)

$$E_y = \sin\left(\frac{\pi x}{a}\right)\exp(-\gamma_{1a}z) + \sum_{\substack{l=1 \\ (\text{odd})}}^{\infty} A_l \sin\left(\frac{l\pi x}{a}\right)\exp(\gamma_{la}z), \quad \text{for } z < 0 \quad (1)$$

Manuscript received July 12, 1976; revised October 21, 1976. This paper is based on work performed for the author's Master's thesis in the Department of Electrical Engineering, University of Akron, Akron, OH.

The author is with the ElectroScience Laboratory, Ohio State University, Columbus, OH.

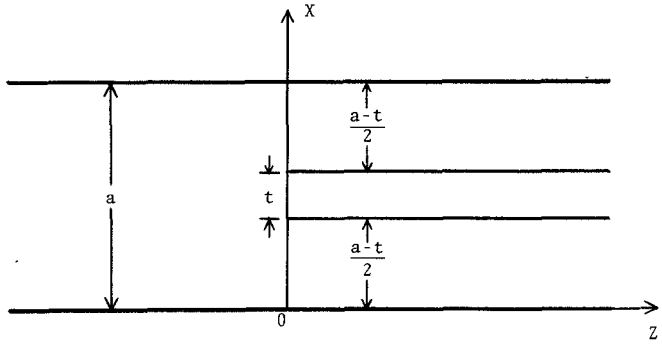

Fig. 2. H-plane bifurcation geometry and coordinate system.

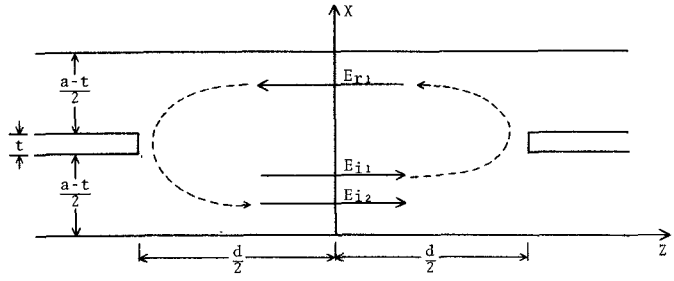

Fig. 3. Ray diagram and coordinate system for the rectangular open-ended cavity.

where

$\gamma_{1a} = \sqrt{(l\pi/a)^2 - k_0^2}$ is the propagation constant;

$k_0^2 = \omega^2\mu_0\varepsilon_0$;

and

γ_{1a} is positive imaginary (propagating mode);

γ_{la}, $l > 1$ is positive real (evanescent mode).

For $z > 0$, $0 < x < (a - t)/2$,

$$E_y = \sum_{l=1}^{\infty} B_l \sin \frac{2l\pi}{(1 - t/a)} \left(\frac{x}{a}\right) \exp(-\gamma_{lb} z) \quad (2)$$

with $\gamma_{lb} = \sqrt{(2l\pi/(a - t))^2 - k_0^2}$. For $(a - t)/2 < x < a$ replace (x/a) by $(1 - x/a)$. $E_y = 0$ for $(a - t)/2 < x < (a + t)/2$, $z > 0$. A_l, B_l are the coefficients of the backward- and forward-scattered modes, respectively. The magnetic fields can be found from

$$H_x = \frac{-j}{\omega\mu_0} \frac{\partial}{\partial z} E_y \quad (3)$$

$$H_z = \frac{j}{\omega\mu_0} \frac{\partial}{\partial x} E_y. \quad (4)$$

The condition of continuity of tangential fields (E_y, H_x) at $z = 0$ leads to a doubly infinite set of equations for the coefficients A_l, B_l. The set is simplified and solved in the manner given by Wexler [5], and can be shown to be equivalent to a moment method solution of an integral equation description of the bifurcation problem. Truncation of the set of equations to a finite size then allows computation of the unknown coefficients by standard Gauss–Jordan elimination. This truncation corresponds to expanding the kernel and aperture field of the equivalent integral equation formulation in a finite Fourier series and, as Mittra *et al.* [8] have shown, using the correct ratio of these two expansion sizes insures satisfaction of the edge condition.

This method gives quickly converging solutions, with the values for A_l, B_l computed with 10 modes differing by less than 1 percent from values obtained when 40 modes are used.

Note that A_1 is the dominant mode reflection coefficient ρ, which is of unit magnitude and, say, phase ϕ.

III. Resonance Condition

The ray diagram of Fig. 3 is used to establish a condition for resonance. The x axis in Fig. 3 is shifted a distance of $-d/2$ from that of Fig. 2 to make the cavity geometry symmetric about $z = 0$. Effects of evanescent modes excited from one of the vanes and impinging on the other vane are assumed to be negligible. The incident TE_{10} wave is assumed to have a unit amplitude and is labeled E_{i1}. E_{i1} travels in the $+z$ direction, reflects from the right-hand termination, and is then labeled E_{r1}, traveling in the $-z$ direction. Wave E_{r1} then reflects from the left termination and becomes E_{i2}, traveling again in the $+z$ direction. If resonance is to occur, E_{i2} must reinforce E_{i1}. Since a lossless cavity is assumed, $E_{i1} = E_{i2}$, or

$$\exp(-j\beta z) = \exp[-j(\beta z + 2\beta d - 2\phi)], \qquad \gamma_{1a} = j\beta \quad (5)$$

where ϕ is the phase of ρ ($\rho = A_1 = \exp(j\phi)$). Solving for d gives

$$d = \frac{\phi + n\pi}{\beta}, \qquad n = 0, 1, 2 \cdots. \quad (6)$$

Equation (6) gives the vane separation d required for resonance at a given frequency in the TE_{10m} mode, where $m = n + 1$. Results for various modes, vane thicknesses, and wavelengths are given in Figs. 4 and 5.

Two X-band cavities were constructed and measured. A comparison of experimental and theoretical data is given in Table I.

IV. Field Expressions

Expressions for the complete $\bar{E}$ and $\bar{H}$ fields for the rectangular open-ended cavity can now be written with reference to the coordinate system of Fig. 3. The dominant mode contribution consists of two waves, one traveling in the positive z direction and the other in the negative direction; evanescent modes are excited at both terminations. By superposition, the y component of the electric field for the TE_{10m} ($m = n + 1$) mode can be obtained. Thus for $-d/2 < z < d/2$, $0 < x < a$,

$$E_y = 2 \exp(j\phi/2) \sin\left(\frac{\pi x}{a}\right) \cos\left(\beta z - \frac{n\pi}{2}\right) + \sum_{\substack{l=3 \\ (\text{odd})}}^{\infty} A_l \sin\left(\frac{l\pi x}{a}\right) \cdot \exp\left(-\gamma_{la}\frac{d}{2}\right) \cdot [\exp(\gamma_{la} z) + (-1)^n \exp(-\gamma_{la} z)]. \quad (7)$$

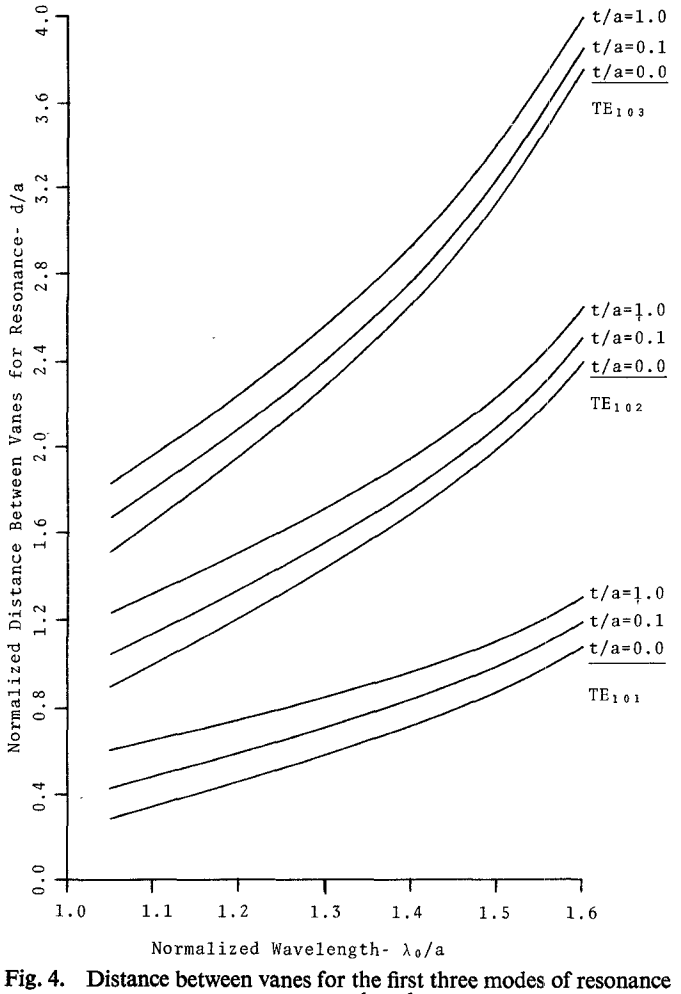

Fig. 4. Distance between vanes for the first three modes of resonance versus wavelength.

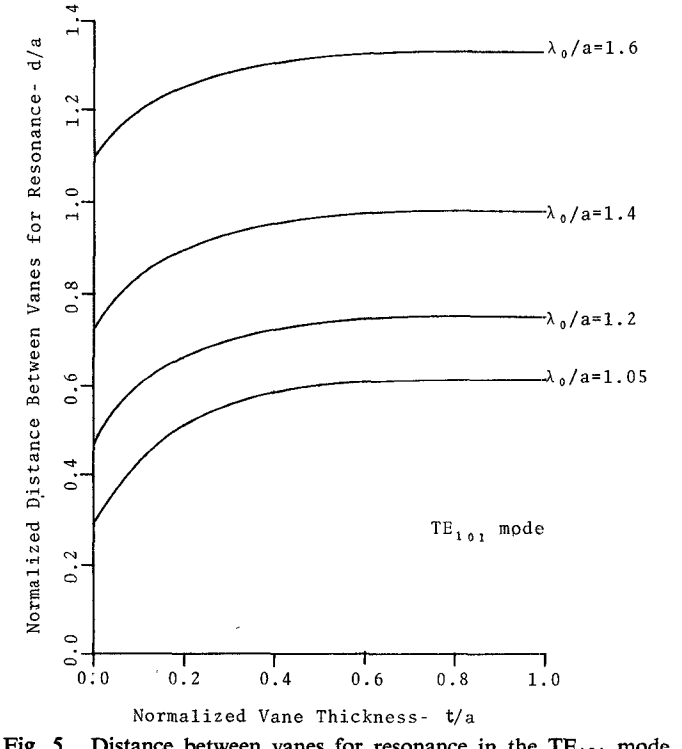

Fig. 5. Distance between vanes for resonance in the TE_{101} mode versus vane thickness.

TABLE I
COMPARISON OF MEASURED AND CALCULATED VALUES OF d/a

MODE	t/a	λ_0/a	meas. d/a	calc. d/a	% error
TE_{101}	.208	1.428	0.924	0.935	1.2%
TE_{103}	.0347	1.405	2.733	2.755	0.8%

For $z > d/2$, $0 < x < (a - t)/2$,

$$E_y = \sum_{l=1}^{\infty} B_l \sin \frac{2l\pi x}{a(1 - t/a)} \exp\left[-\gamma_{lb}(z - d/2)\right]. \quad (8)$$

For $z < -d/2$, $0 < x < (a - t)/2$,

$$E_y = (-1)^n \sum_{l=1}^{\infty} B_l \sin \frac{2l\pi x}{a(1 - t/a)} \exp\left[\gamma_{lb}(z + d/2)\right]. \quad (9)$$

For $(a + t)/2 < x < a$ replace (x/a) by $(1 - x/a)$.

A constant phase factor of $\exp(-j\beta d/2)$ was dropped from (7)–(9). As was mentioned previously, the H_x and H_z fields can quickly be found from relations (3) and (4). These expressions yield a complex function of x and z, but it is such that the phase is constant with respect to position and thus can be removed. To within an overall phase factor, this allows plotting the $\bar{E}$ and $\bar{H}$ fields versus position. Figs. 6–8 show three-dimensional plots of E_y, H_x, and H_z versus position for the TE_{101} resonant mode. The magnetic field singularities can easily be recognized. These plots were made using 20 modes in the modal expansion.

V. ENERGIES AND Q

The average stored electric and magnetic energies are found from the relations

$$W_e = \frac{\varepsilon_0}{4} \iiint \bar{E} \cdot \bar{E}^* \, dv$$

$$W_m = \frac{\mu_0}{4} \iiint \bar{H} \cdot \bar{H}^* \, dv.$$

Due to the symmetry of the cavity, only one-fourth of the total volume need be integrated. These energies were evaluated using expressions (7) and (8), together with (3) and (4). This calculation, carried out elsewhere [7], is too lengthy to repeat here.

The result of this computation gives a quickly converging electric energy while the magnetic energy converges slightly slower, with increasing number of modal expansion modes. The energies agree to within 1 percent after using only 10 modes. Agreement of the electric and magnetic energies is a convenient analysis check.

The power lost per cycle due to ohmic losses in the cavity walls is found by the standard perturbation method, as in Collin [6], where the lossy cavity fields are taken to be identical to the lossless cavity fields. Thus

$$P_l = \frac{R_m}{2} \iint |H_{\tan}|^2 \, dS$$

where $R_m = \sqrt{\omega\mu_0/2\sigma}$ and σ is the conductivity of cavity.

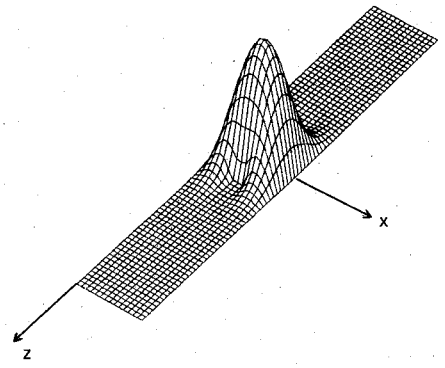

Fig. 6. Electric field E_y versus position for the TE_{101} mode. $\lambda_0/a = 1.4$, $t/a = 0.2$, $0 < x < a$, $-3a < z < 3a$.

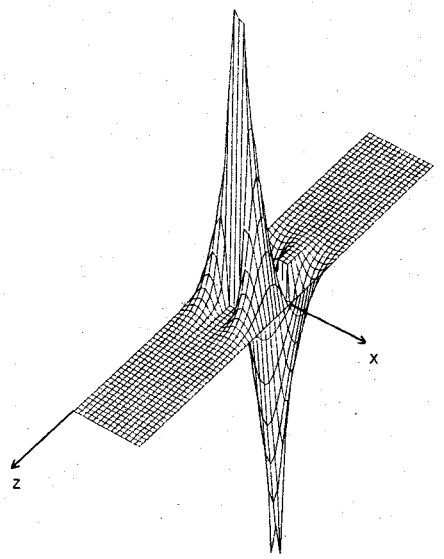

Fig. 7. Magnetic field H_x versus position for the TE_{101} mode. $\lambda_0/a = 1.4$, $t/a = 0.2$, $0 < x < a$, $-3a < z < 3a$.

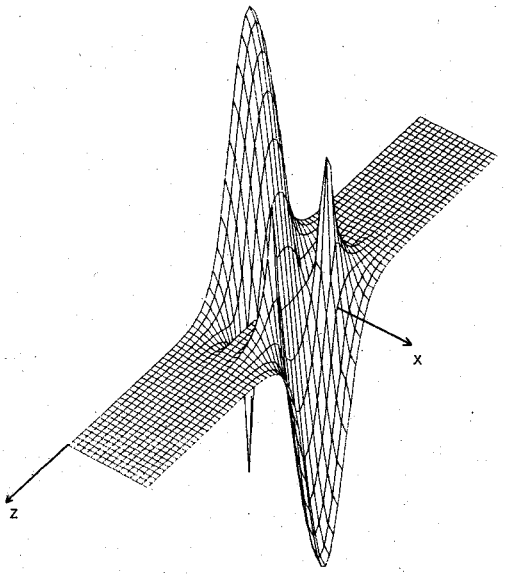

Fig. 8. Magnetic field H_z versus position for the TE_{101} mode. $\lambda_0/a = 1.4$, $t/a = 0.2$, $0 < x < a$, $-3a < z < 3a$.

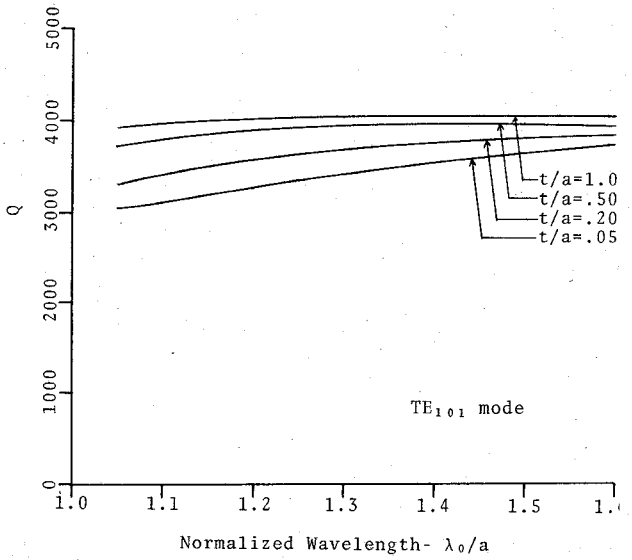

Fig. 9. Unloaded cavity Q versus wavelength for the TE_{101} mod

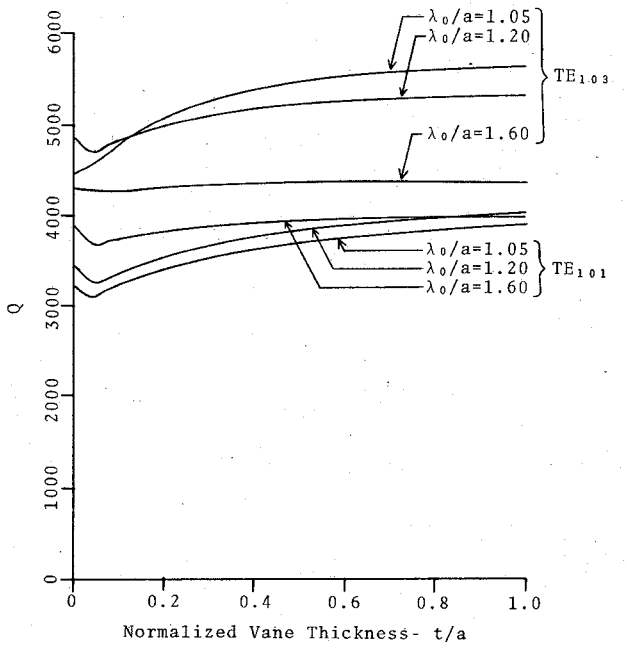

Fig. 10. Unloaded cavity Q versus vane thickness for the TE_{101} an TE_{103} modes.

Calculation of P_l is also tedious, and will not be repeated here; the details may be found in [7]. This calculation is further complicated by the fact that the waveguide modes are not all orthogonal on the cavity surfaces, meaning that mode coupling is present which increases P_l. Unloaded cavity Q is found from the expression

$$Q = \frac{\omega(W_e + W_m)}{P_l}.$$

The power loss term is not highly convergent, and increases by as much as 15 percent as the number of modes used is increased from 10 to 40. The source of this poor convergence was traced to terms in P_l which account for losses at the vane edge. It is felt that this problem is caused

by H_x and H_z being singular[1] at the vane edges, making the surface currents and hence the power loss at these locations quite large. Of course, in the practical cavity the conductivity is not perfect and the fields would not be singular. Also, better convergence is obtained with thicker vanes, for which the fields are better behaved. Results of this Q calculation are presented in graphical form in Figs. 9 and 10. It is estimated that the calculated Q results are better than ± 10 percent accurate for $t/a < 0.1$ and better than ± 5 percent for $t/a > 0.1$. A useful check on the Q calculation is possible when $t/a = 1.0$. In this case the cavity is no longer open ended and is a simple closed rectangular cavity for which the Q is easily calculated [6] and found to agree with the results from this analysis. Note that the Q of the rectangular open-ended cavity is lower than the Q of a closed cavity of the same resonant frequency. The Q of the two constructed cavities was measured and found to be significantly lower (~ 60 percent) than the theoretical Q. This difference, which is quite common, is accounted for by the coupling hole size (0.2 in) and the surface finish, which was not polished or even very smooth.

VI. Conclusion

A field analysis of rectangular open-ended cavities has been presented. The resonant frequency and Q have been derived and presented in graphical form. Expressions for the fields inside the cavity were written and plotted in three dimensions. Good accuracies were obtained in the resonant frequency calculation; however, the Q calculation was not as well behaved due to the power loss becoming large at the vane edge. Comparisons of theoretical and experimental results for two constructed cavities were given.

Topics for further work include improvement of the Q calculation and quantifying the effect of a coupling hole on the cavity frequency and Q. Variations in the cavity design such as unsymmetrical terminations or more than one vane in each termination region could also be investigated.

[1] As a reviewer has pointed out, only H_z is strictly singular while H_x has a step change equal to J_s at the discontinuity.

References

[1] R. O. Gilmer and D. C. Thorn, "Some design criteria for open-ended microwave cavities," Univ. New Mexico, Albuquerque, Tech. Rept. EE-65, June 1962.

[2] N. C. Wenger, "Resonant frequency of open-ended cylindrical cavity," *IEEE Trans. Microwave Theory Tech.*, vol. MTT-15, pp. 334–340, June 1967.

[3] R. E. Collin, *Field Theory of Guided Waves.* New York: McGraw-Hill, 1960, pp. 447–449.

[4] R. Mittra and S. Lee, *Analytical Techniques in the Theory of Guided Waves.* New York: Macmillan, 1971, pp. 30–45.

[5] A. Wexler, "Solution of waveguide discontinuities by modal analysis," *IEEE Trans. Microwave Theory Tech.*, vol. MTT-15, pp. 508–517, Sept. 1967.

[6] R. E. Collin, *Foundations for Microwave Engineering.* New York: McGraw-Hill, 1966, pp. 324–325.

[7] D. M. Pozar, "Field analysis of an open-ended rectangular microwave cavity," M.S. thesis, University of Akron, Akron, OH, June 1976.

[8] R. Mittra, T. Itoh, and T. S. Li, "Analytical and numerical studies of the relative convergence phenomenon arising in the solution of an integral equation by the moment method," *IEEE Trans. Microwave Theory Tech.*, vol. MTT-20, pp. 96–104, Feb. 1972.

Ferrite Planar Circuits in Microwave Integrated Circuits

TANROKU MIYOSHI, MEMBER, IEEE, S. YAMAGUCHI, AND SHINJI GOTO

Abstract—**The ferrite planar circuit to be discussed in this paper is a general planar circuit using ferrite substrates magnetized perpendicular to the ground conductors. The main subject of this paper is the analysis of an arbitrarily shaped triplate ferrite planar circuit. In particular, the circuit parameters of the equivalent multiport are determined. To analyze ferrite planar circuits in general, two approaches are possible. One approach is based upon a contour-integral solution of the wave equation. In the other approach the fields in the circuit are expanded in terms of orthonormal eigenfunctions. Examples of the application of such analyses are described.**

Manuscript received September 7, 1976; revised December 17, 1976.
The authors are with the Department of Electronic Engineering, Kobe University, Kobe, Japan.

I. Introduction

THE planar circuit is defined as an electrical circuit whose thickness in one direction is much less than one wavelength and whose dimensions in the orthogonal directions are comparable to the wavelength. The concept of the planar circuit was proposed by Okoshi in 1969 [1]. Since then, its analysis [2]–[5] and synthesis [6], [7] have been investigated for many circuits using isotropic material for the spacer.

This paper will present the general treatment of a planar circuit using ferrite material for the spacer. In particular, an arbitrarily shaped ferrite planar circuit is discussed. The